

## Original Article

# Endothelial progenitor cells with stem cells enhance osteogenic efficacy

Qiong Li<sup>1\*</sup>, Tao Yu<sup>2\*</sup>, Fang Wang<sup>1</sup>, Xin Liu<sup>1</sup>, Zuolin Wang<sup>1</sup>

<sup>1</sup>Department of Oral Implantology, School & Hospital of Stomatology, Tongji University, Shanghai Engineering Research Center of Tooth Restoration and Regeneration, Shanghai 200072, China; <sup>2</sup>Department of Orthopedic Surgery, Tongji Hospital, Tongji University School of Medicine, Shanghai 200065, China. \*Equal contributors and co-first authors.

Received October 24, 2019; Accepted May 18, 2020; Epub June 15, 2020; Published June 30, 2020

**Abstract:** Background: Mesenchymal stem cell (MSC)-based bone tissue engineering is a promising treatment option for maxillary sinus augmentation. Rapid vascularization is necessary to enhance the osteoinductive efficacy and prevent necrosis of the tissue-engineered bone. This study investigated whether the co-autotransplantation of endothelial progenitor cells (EPCs) could significantly enhance the *in vivo* osteogenic efficacy of MSCs and prevent necrosis of the tissue-engineered bone in a maxillary sinus augmentation model in dogs. Methods: We evaluated the *in vitro* osteogenic activities of a clinically-used scaffold-deproteinized bovine bone (Bio-Oss) by examining cell adhesion and alkaline phosphatase (ALP) activity. *In vivo*, sinus augmentations were performed identically on both sides of dogs (n = 3 per group) using three treatment groups: (A) Bio-Oss with MSCs and EPCs; (B) Bio-Oss with MSCs; and (C) Bio-Oss with EPCs. The tissue implants were evaluated 24 weeks post-implantation. Results: *In vitro*, co-application of EPCs and MSCs on Bio-Oss significantly enhanced adhesion and ALP activity. *In vivo*, co-autotransplantation of MSCs and EPCs resulted in a significantly higher height, compressive strength, bone volume density, trabecular thickness, and trabecular number and a significantly lower trabecular separation compared with the other groups. The fluorescent test showed co-autotransplantation caused a significantly higher mineral apposition rate than the other groups. Histomorphometric analysis showed co-application resulted in the highest rate of new bone formation. Newly formed bone was frequently in the center of the implants with EPCs and MSCs, but not the other implants. Conclusions: Co-autotransplantation of EPCs and MSCs significantly enhanced the *in vivo* osteogenic efficacy, suggesting promising potential for sinus augmentation.

**Keywords:** Endothelial progenitor cells, mesenchymal stem cells, bone marrow stromal cells, osteogenesis, angiogenesis, tissue-engineered bone

## Introduction

Bone height in the posterior maxilla may be limited because of the loss of maxillary teeth and progressive pneumatization of the basal sinus with formation of caudal recesses [1]. Thus, placement of dental implants in the atrophic posterior maxilla is a challenging procedure. The sinus augmentation technique was first presented in the late 1970s by Tatum and is now the most common procedure in implant reconstructive surgery [2]. Autogenous bone grafts, allografts, xenografts, and synthetic materials have been explored for this surgical procedure. Autogenous bone is considered the gold standard grafting material because of its

osteoinductive and osteoconductive properties, but the use of autogenous bone has a risk of donor site morbidity (infection, pain, and loss of function) and unpredictable graft resorption [3]. Therefore, various bone substitutes are used. A bone substitute of bovine origin (Bio-Oss, Geistlich Pharma Wolhusen, Switzerland) with osteoconductive properties and high biocompatibility is frequently used for augmentation, either alone or in combination with autogenous bone [4-6]. The anorganic bone matrix of Bio-Oss appears to have a microporous structure similar to human cancellous bone [7]. This alternative material has no osteoinductive potential, so it requires more time for bone healing [8].

## Endothelial progenitor cells with stem cells improve osteogenesis

The engineering of bone tissue offers new therapeutic strategies for the repair and regeneration of bone defects for maxillary sinus augmentation [9, 10]. Bone marrow stromal cells (BMSCs) are a particularly attractive source for osteogenic precursors for bone tissue engineering [11], because they easily expand in culture and differentiate into cells with an osteogenic phenotype. However, tissue-engineered bone requires not only cell populations capable of creating new bone and a biocompatible scaffold, but also formation of an appropriate vascular bed to support the metabolic needs of bone. If adequate perfusion cannot be established quickly, central necrosis of the newly produced bone tissue will occur [12]. Thus, vascularization becomes the cornerstone of the healing process in large volume tissue-engineered bone.

Endothelial precursor cells (EPCs), progenitor cells able to initiate neovascularization, were initially identified by Isner and Asahara in 1997 [13]. Compared with mature endothelial cells (ECs), EPCs have an exciting angiogenic, proliferative, and survival potential *in situ*. EPCs occur in low numbers, but when expanded in culture can undergo more than 1000 population doublings, in sharp contrast to mature ECs that senesce after 30 population doublings [14]. EPCs are derived from bone marrow, circulate in the peripheral blood, and play a crucial role in the repair or formation of blood vessels [13]. Han shows that late-outgrowth EPCs express markers associated with pluripotency and can directly express an osteogenic phenotype under bone differentiation conditions *in vitro* [15]. For these reasons, researchers have turned to the study of co-culture interactions with EPCs in the hope of gaining insight into the vascularization process. Steiner shows that *in vitro*, T17b EPCs stimulate mesenchymal stem cell (MSC) proliferation, but not vice versa. On the other hand, MSCs promote the survival of EPCs [16].

The aim of this study was to investigate whether the addition of EPCs could improve osteogenesis and prevent necrosis of tissue-engineered bone *in vivo* through efficient neovascularization. We established a co-cultured system of MSC-derived osteogenic cells and EPCs. Using a large animal canine model, we explored the effect of maxillary sinus augmentation

using a tissue engineered bone of Bio-Oss and the co-cultured cells.

### Material and methods

#### *Experimental animals*

Six adult beagle dogs in healthy condition, aged 18 months old with an average weight of 12.5 kg were used as a cell source for MSCs and EPCs in this study. The experimental protocol was approved by the Animal Care and Experiment Committee of Tongji Hospital affiliated with Shanghai Tongji University, School of Medicine.

#### *Isolation and culture of mesenchymal stem cells and endothelial progenitor cells from dog bone marrow*

MSCs and EPCs were harvested and cultured independently using a similar technique except for the materials and the culture media. After performing general anesthesia on the dogs using an intravenous injection of pentobarbital Nembutal 3% (30 mg/kg), bone marrow (BM) was aspirated from the dogs' iliac crest. MSCs were isolated according to the method previously reported [17]. Mononuclear cells (MNCs) were isolated from all heparinized BM aspirates by density gradient centrifugation using Ficoll Paque Plus (GE Healthcare, Uppsala, Sweden). Separation was achieved by centrifugation at 400 g for 30 min. The MNCs were then washed in PBS and cultured in culture flasks (Corning, New York, USA) with  $\alpha$ -MEM (HyClone, Logan, USA) containing 10% (V/V) fetal bovine serum (GIBCO, Carlsbad, USA). Cells were incubated at 37°C in a humidified 5% CO<sub>2</sub> incubator and the medium was changed twice weekly. When primary cultures reached 70%-80% confluency, attached cells were passaged by exposure to 0.25% trypsin/EDTA (GIBCO) for 3 min and reseeded at a density of  $1 \times 10^5$  cells/cm<sup>2</sup> in the culture flasks. BM-EPCs were isolated using the technique previously reported [12]. Briefly, MNCs isolated by the density gradient method using Ficoll-Paque Plus were plated in disposable culture flasks coated with fibronectin and cultured in endothelial cell growth medium-2 (Lonza, Basel, Switzerland). After 3 days of culture, nonadherent cells were removed and new medium was supplied. The culture was maintained until 70%-80% confluency. The adherent

## Endothelial progenitor cells with stem cells improve osteogenesis

cells were released using 0.25% trypsin/EDTA and reseeded onto tissue culture flasks for subsequent passages. MSCs and EPCs at passage 2-3 were used for the following experiments.

### *In vitro differentiation of mesenchymal stem cells*

We studied the *in vitro* multi-differentiation potential of the MSCs toward osteogenesis, adipogenesis, and chondrogenesis. For osteogenic differentiation, passage 2 MSCs with a density of  $1 \times 10^3$  cells/cm<sup>2</sup> were added to 6-well culture plates in  $\alpha$ -MEM containing 10% (V/V) fetal bovine serum. After one day, the medium was changed to osteogenic medium. The osteogenic medium was dog mesenchymal stem cell osteogenic differentiation medium (Cyagen Biosciences, Santa Clara, USA). The medium was changed twice weekly. After 3 weeks, ALP activity was assayed using a BCIP/NBT ALP color development kit (Beyotime Institute of Biotechnology, Haimen, China). Calcium deposits were detected by staining with 2% Alizarin Red S (Sigma, Shanghai, China). For adipogenic differentiation, passage 2 MSCs with a density of  $2 \times 10^4$  cells/cm<sup>2</sup> were added to 6-well culture plates in  $\alpha$ -MEM containing 10% (V/V) fetal bovine serum. After 3-5 day, the medium was changed to dog mesenchymal stem cell adipocyte differentiation medium (Cyagen Biosciences, Santa Clara, USA). The medium was changed twice a week. Oil red O (Sigma) staining was performed to analyze adipogenesis after 4 weeks. For chondrogenic differentiation, passage 2 MSCs with a density of  $5 \times 10^5$  cells/cm<sup>2</sup> were added to 15 ml polypropylene culture tubes in chondrogenic differentiation medium (Cyagen Biosciences). The cell pellets were fed every 3 days by completely replacing the medium in each tube. After 28 days, pellets were formalin fixed and paraffin embedded for Alcian blue staining.

### *Immunocytochemistry*

Cells of an endothelial lineage that attach as spindle-shaped cells and co-stain with 1'-dioctadecyl-3,3,3',3'-tetramethylindocarbocyanine perchlorate-labeled acetylated low-density lipoprotein (Dil-Ac-LDL) and fluorescein isothiocyanate-conjugated ulex europaeus lectin (FITC-UEA-I) were identified as EPCs. The cells were observed under a fluorescent microscope (Olympus, Tokyo, Japan).

### *Flow cytometry analysis*

Passage 2 MSCs and BM-EPCs were placed in FACS tubes (BD Biosciences, San Jose, USA) at  $2 \times 10^5$  cells/tube, washed with FACS buffer (PBS containing 1% sodium azide and 1% FBS, pH 7.2). MSCs were incubated with antibodies including CD34-PE (eBioscience, San Diego, USA), CD29-PE (Abcam, Cambridge, UK), and CD44-FITC (eBioscience) at room temperature for 1 h, while BM-EPCs were incubated with antibodies including CD34-PE (eBioscience), CD133-FITC (eBioscience), and VEGFR-2 (Abcam) at room temperature for 1 h. Cells were washed twice with FACS buffer and resuspended in 500  $\mu$ l of FACS buffer. BM-EPCs incubated with VEGFR-2 were incubated with anti-rat IgG secondary antibodies labeled with FITC for 1 h, and then washed twice with FACS buffer and resuspended in 500  $\mu$ l of FACS buffer. Cell fluorescence was evaluated by flow cytometry.

### *Preparation of Bio-Oss and co-culture of MSCs and EPCs*

Bio-Oss granules (Geistlich Pharma, Wolhusen, Switzerland) were prepared and sterilized with ethylene oxide for cell cultures. After placement in the culture plates, Bio-Oss granules were coated with fibronectin (10 mg/ml) for at least 1 h at 37°C. For cell seeding, MSCs were cultured in osteogenic media for 3 days prior to co-culture. Then, MSCs were mixed with EPCs at the same density of  $2 \times 10^6$  cells/ml in a 1:1 mixture of osteogenic and angiogenic medium (EGM-2). Cells in suspension were slowly combined with Bio-Oss granules until saturation. For control conditions, monocultures of MSCs and EPCs in their normal respective media were seeded onto the Bio-Oss granules at a density of  $2 \times 10^6$  cells/ml.

### *Cell adhesion on Bio-Oss granules*

MSCs-derived osteogenic cells alone, EPCs alone, and the co-cultured cells at the same density of  $2 \times 10^6$  cells/ml were dripped on the Bio-Oss granules layer and incubated for 3, 6, and 12 h at 37°C. After incubation, the medium containing the non-adhering cells was removed and rinsed over the Bio-Oss granules layer. This procedure was repeated three times and the remaining cells in the supernatant were counted. Then, these granules were transferred to another well and the cells on the bottom of the

## Endothelial progenitor cells with stem cells improve osteogenesis

initial seeding well were counted. The percentage of adherent cells was calculated:  $[(\text{initial cell number} - \text{remaining cell number}) / \text{initial cell number}] \times 100\%$ .

### *Scanning electron microscopy observation and alkaline phosphatase activity assay in the co-cultured cells*

After 7 days, the Bio-Oss granules with MSCs-derived osteogenic cells alone and EPCs alone were fixed in 2% glutaraldehyde for 2 h and the morphology was observed using a Hitachi S-3400N scanning electron microscope.

To quantify the mineralization in the cultures, an ALP substrate kit (Wako, Saitama, Japan) was used for the Bio-Oss granules with cells for 24 h, 3 days, 7 days, and 14 days according to the manufacturer's instruction. In brief, the Bio-Oss granules with cells were washed with PBS, and the cells were lysed using 0.05% Triton X-100 (Sigma). After centrifugation at 15000 rpm for 10 min at 4°C, 20 µl supernatant sample was extracted from each sample and added to 100 µl freshly prepared substrate solution (para-nitrophenylphosphate solution). The mixture was shaken for 1 min using a plate mixer and incubated at 37°C for 15 min. The enzymatic reaction was stopped by adding 80 µl stop solution (0.2 mol/l sodium hydroxide solution). Serial dilutions of para-nitrophenol solution served as standards. The absorption was measured at a wavelength of 405 nm. The results from ALP activity analyses were expressed in nanomoles (nmol) of p-nitrophenol produced per minute.

### *Surgical procedure and preparation of the specimens*

Eight weeks after tooth extraction and complete healing of the edentulous ridge, the dogs were anesthetized as described. The floor elevation procedure and implant placement were performed identically on both sides of each animal according to the technique described by Haas [18]. Each dog sinus was randomly selected to receive one of the three following materials: Group A comprised of scaffold Bio-Oss/MSCs-derived osteogenic cells and EPCs (n = 3); Group B comprised of scaffold Bio-Oss/MSCs-derived osteogenic cells (n = 3) as a control group; or Group C comprised of scaffold Bio-Oss/EPCs (n = 3) as a control group.

A single surgeon performed all surgeries. Briefly, a skin incision below the lower eyelid was made to expose the lateral maxillary sinus wall. A round bur was used to create a 1×1.5-cm opening in the lateral wall of the maxillary sinus. After removing the bone, the sinus membrane was carefully elevated from the sinus floor to avoid perforations. The space between the sinus membrane and the sinus floor was filled with 1 ml bone substitute to elevate the sinus with an average height of 10 mm from the sinus floor. Then, the periosteum and skin flap were repositioned and sutured. After surgery, all dogs recovered well.

The time course of new bone formation and mineralization was assessed by sequential fluorochrome labeling. The animals were intraperitoneally administered 25 mg/kg hydrochloride tetracycline (TE, Sigma), 20 mg/kg calcein (CA, Sigma), and 30 mg/kg Alizarin Red S (AL, Sigma), at 4, 12, and 20 weeks after the operation.

The dogs were sacrificed 24 weeks after surgery. Maxillofacial CT images were acquired using Cone beam CT (CBCT) with 60 kV voltage tension and 3 mA ampere, 0.96 mm slice thickness. The implants could be distinguished from original bone by density and structure. The implants were retrieved and immediately used for micro-CT. Each augmented maxillary sinus was dissected into two parts by the sagittal plane in the mesiodistal direction. The mean height value of four specimens in each group, defined as the maximal perpendicular distance between the floor and the top of the augmented maxillary sinus [19], was measured using a Vernier caliper. One part of each specimen was used for the microhardness test and then fixed in 10% buffered formalin (pH 7.4). This part was further decalcified and embedded in paraffin for immunohistochemical detection. The other undecalcified part was embedded in polymethylmethacrylate (PMMA) and cut in 10-µm thick sections using a microtome (Leica, Wetzlar, Germany) for histomorphometrical examination.

### *Micro-CT examination of the maxillary sinus*

The implants were scanned using a SkyScan-1176 Micro-CT (Micro Technology Hong Kong Ltd., Kontich, Belgium). This region included 1200 images with a resolution of 1068×1068

## Endothelial progenitor cells with stem cells improve osteogenesis

pixels. This system was set to 65 kV, 385  $\mu$ A, and 250 ms exposure time. The three-dimensional images were obtained for qualitative and quantitative evaluation ( $\sigma = 1.2$ , support = 1, threshold for bone = 255, and threshold for graft = 95). The volume of interest (VOI) was selected at the center of the graft with a 3 $\times$ 4 mm area. The following microarchitecture parameters were assessed: bone volume to total volume ratio (BV/TV), connectivity density (Conn.Dn), trabecular thickness (Tb.Th), trabecular separation (Tb.Sp), and trabecular number (Tb.N). BV/TV indicates the portion of mineralized tissue, Conn.Dn indicates the degree of trabecular branching, and Tb.Th, Tb.Sp, and Tb.N provide detailed information on the thickness, organization, and amount of trabecular.

### *Microhardness test*

Microhardness measurements were performed on eight locations previously designated for each specimen by the indentation method (DHV-1000, Shanghai Shangcai Testing Machines Co., Ltd., Shanghai, China) according to the method previously reported [20]. In brief, 25 g was loaded with dwell time of 20 seconds and the average compressive strength was calculated for each group, expressed as hardness Vickers degree (HV).

### *Histological examination for the undecalcified parts*

The undecalcified parts were observed for fluorescent labeling using confocal laser scanning microscope (Leica TCS SP5 II). The hydrochloride tetracycline yellow, Calcein green, and Alizarin red were detected at 405/580 nm, 488/517 nm, and 543/617 nm excitation/emission wavelengths respectively. The kinetic histomorphometric parameter was performed using an image analysis system (Image-Pro Plus, Media Cybernetics, Rochville, USA): mineral apposition rate (MAR,  $\mu$ m/day) was calculated.

### *Histomorphometrical evaluation for the decalcified parts*

The decalcified parts were embedded in paraffin and cut into 4- $\mu$ m sections. The sections were stained with hematoxylin-eosin. To determine the extent of the fully mineralized bone, anti-osteocalcin antibody (Abcam) was used for

immunofluorescent staining. Five random fields of each section were pictured. Image quantifications were performed using Image-Pro Plus software.

### *Statistics*

All the quantitative measurements were presented as mean  $\pm$  standard deviation (Mean  $\pm$  SD). Statistical analyses were performed using the statistics software package SPSS 17.0 for Windows. Comparisons between groups in cell adhesion, ALP activity, height of augmented maxillary sinus, microarchitecture parameters, new bone formation, and remnant particles were analyzed via ANOVA followed by a Student-Newman-Keuls post hoc test. Mann-Whitney U-test for non-parametric procedures was used to determine microhardness and mineral apposition rate.  $P < 0.05$  was considered statistically significant.

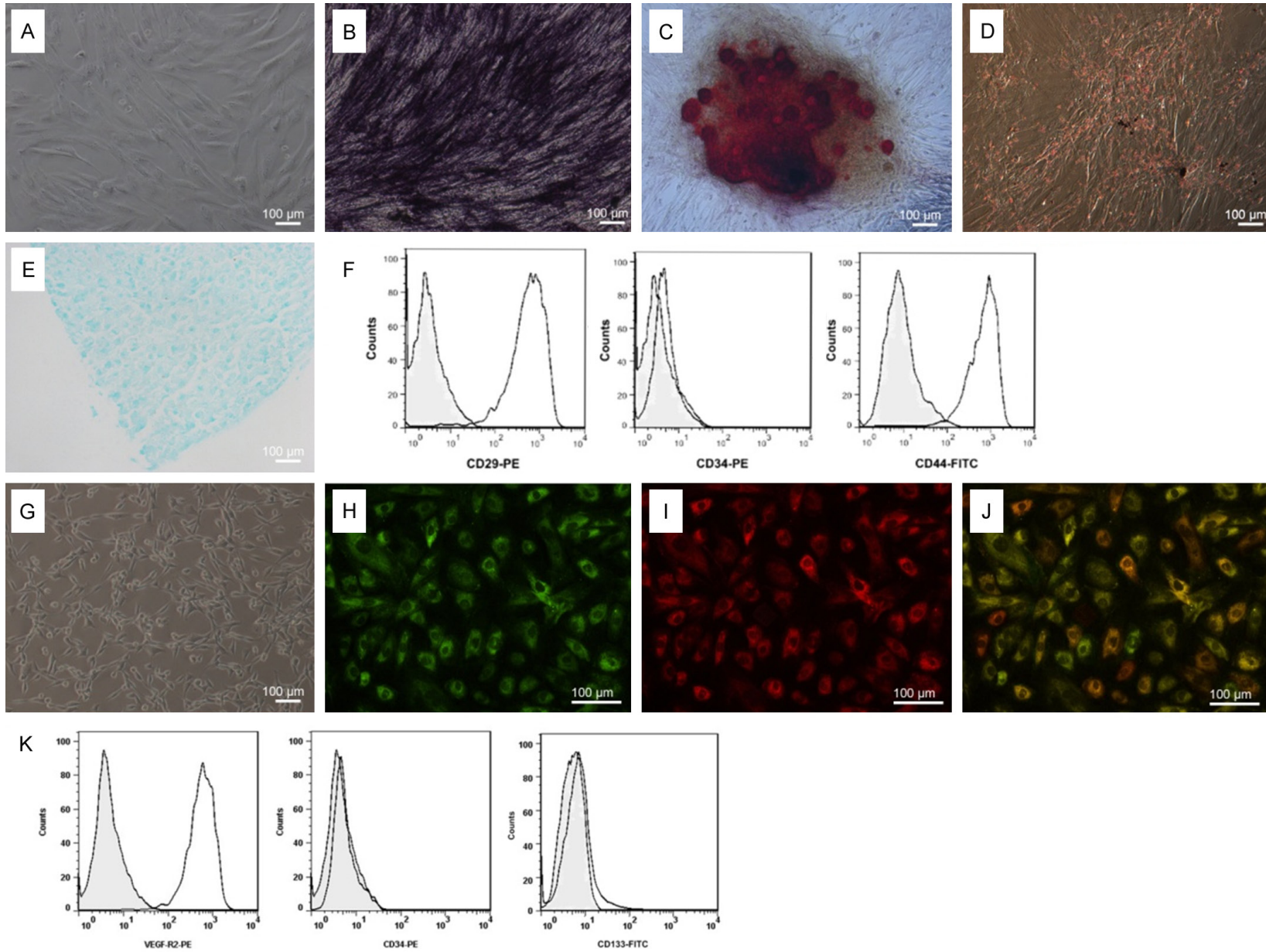
## **Results**

### *Culture and characterization of MSCs and EPCs*

MSCs displayed spindle morphology (**Figure 1A**). We confirmed that MSCs were capable of differentiating into many cell lineages. The osteogenic differentiation assays showed both ALP-positive staining (**Figure 1B**) and mineralized calcium nodules with Alizarin Red S staining (**Figure 1C**) in these cells. The adipogenic differentiation of MSCs was verified by positive Oil Red O staining after 4 weeks of induction (**Figure 1D**). The cells also had the capacity to undergo chondrogenic differentiation demonstrated using Alcian blue staining after induction for 4 weeks (**Figure 1E**). Cell surface antigen phenotype was assessed on MSCs using flow cytometry (**Figure 1F**). Adhesion molecule protein CD29 and receptor molecule protein CD44 were highly expressed on MSCs. MSCs were negative for hematopoietic markers such as CD34.

EPCs displayed a cobblestone-like appearance after 12 days of culture (**Figure 1G**). The cells were positive for FITC-UEA-I and Dil-ac-LDL (**Figure 1H-J**), which are endothelial cell lineage markers of EPCs [21]. Cell surface antigen phenotype was assessed on EPCs using flow cytometry (**Figure 1K**). EPCs displayed a low signal for CD34 and CD133. VEGFR-2 was highly expressed on EPCs.

Endothelial progenitor cells with stem cells improve osteogenesis



## Endothelial progenitor cells with stem cells improve osteogenesis

**Figure 1.** Characterization of mesenchymal stem cells (MSCs) and endothelial progenitor cells (EPCs) used in this study. (A) Canine MSCs at P2 displayed spindle morphology. (B) ALP staining and (C) Alizarin Red S staining verify osteogenic differentiation of MSCs after three weeks of induction. (D) The adipogenic differentiation of MSCs was verified by positive Oil Red O staining after 4 weeks of mass culture and induction. (E) MSCs also had the capacity to undergo chondrogenic differentiation. This was evident through Alcian blue staining after induction for 4 weeks. (F) Flow cytometry analysis of the expression of indicated cell surface markers related to MSCs. (G) Morphology of EPCs at 12 days of culture. EPCs could take up (H) FITC-UEA-1 and bind to (I) Dil-Ac-LDL as shown by the green and red fluorescence. (J) Merged images show that most cells were dual-positive. Dual-positive cells were defined as EPCs. (K) Flow cytometry analysis of the expression of indicated cell surface markers related to EPCs. Scale bar = 100  $\mu$ m.

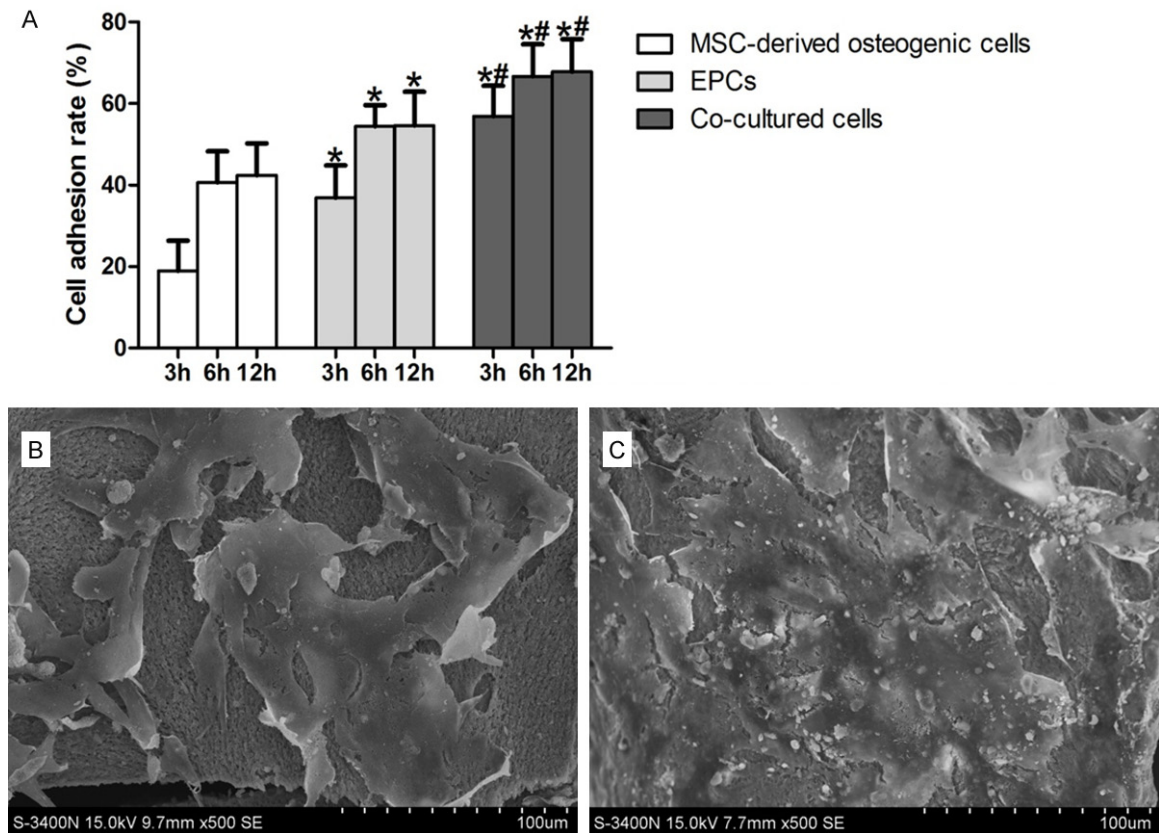


**Figure 2.** MSCs-derived osteogenic cells alone, EPCs alone, and the co-cultured cells at the same density were dripped on the Bio-Oss granules layer and incubated for 3, 6, and 12 h at 37 °C. (A) The percentage of adherent cells was calculated. Results are presented as the mean  $\pm$  SD. \*:  $P \leq 0.05$  vs MSC-derived osteogenic cells, #:  $P \leq 0.05$  vs EPCs. The SEM shows the morphological appearance of (B) MSCs-derived osteogenic cells and (C) EPCs on the Bio-Oss granules after 7 days of culture.

### Cell seeding efficiency on the Bio-Oss granules and SEM evaluation

The co-cultured cells consistently had the highest adhesion rate throughout the observation period. Compared with MSCs-derived osteogenic cells, more EPCs were attached to the Bio-Oss granules at 3 h, 6 h, and 12 h (**Figure 2A**). Interestingly, the number of adhering cells remained constant at 6 h and 12 h.

The SEM showed the morphological appearance of MSCs-derived osteogenic cells (**Figure**

**2B**) and EPCs (**Figure 2C**) on the Bio-Oss granules. After 7 days, MSCs-derived osteogenic cells and EPCs combined well with the scaffolds. The pseudopodia and projections of MSCs-derived osteogenic cells on the Bio-Oss granules still existed. Approximately sixty percent of the scaffolds were covered with MSCs-derived osteogenic cells. Almost all the pseudopodia of EPCs disappeared and the scaffolds were entirely covered with a layer of EPCs. It suggested that the Bio-Oss granules facilitated the adhesion and growth of MSCs-derived osteogenic cells and EPCs.

## Endothelial progenitor cells with stem cells improve osteogenesis

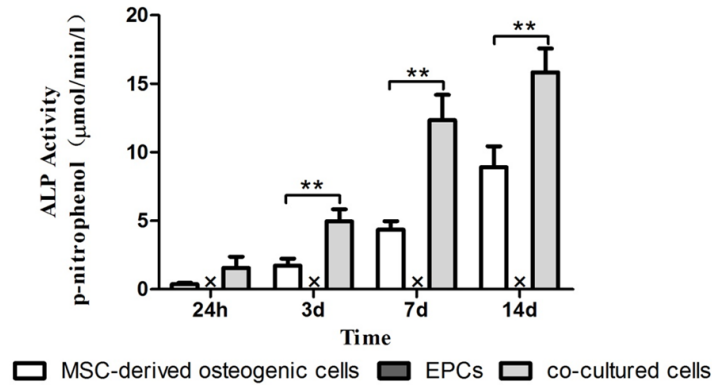


**Figure 3.** ALP activity in the Bio-Oss granules with MSC-derived osteogenic cells, EPCs and co-cultured cells for 24 h, 3 days, 7 days, and 14 days. Results are presented as mean  $\pm$  SD. \*:  $P \leq 0.05$ . x: No expression.

### Assessment of cell osteogenesis on the Bio-Oss granules

ALP activity in the Bio-Oss granules with cells was studied as an early marker of osteogenic differentiation. ALP activity increased gradually in MSC-derived osteogenic cells and co-cultured cells with the Bio-Oss granules. However, the co-cultured cells with the Bio-Oss granules showed higher ALP activity than MSCs-derived osteogenic cells at 24 h, 3 days, 7 days, and 14 days (**Figure 3**). ALP activity of EPCs with the Bio-Oss granules was almost zero.

### The maxillary sinus height analysis and micro-hardness evaluation

The augmented maxillary sinus of each group at 24 weeks post-operation was observed using sagittal maxillofacial CT images (**Figure 4A1-C1**). The augmented maxillary sinus was set as the region of interest and reconstructed by micro-CT (**Figure 4A2-C2**). A 3D reconstruction of the VOI for the three groups showed remnants of Bio-Oss granules (pink) and newly formed bone (white) (**Figure 4A3-C3**). The new bone of the central area in group A was obvious, whereas that in group B and group C formed less. The mean height of each group was measured to evaluate the effects of implants after maxillary sinus augmentation. The height of group A ( $7.54 \pm 0.92$  mm) was significantly higher than group B or group C ( $P < 0.05$ ) (**Figure 4D**). Group B ( $6.04 \pm 0.62$  mm) obtained a higher height than group C ( $4.12 \pm 0.95$  mm).

The biomechanical data revealed that group A exhibited the highest enhancement in the compressive strength ( $558.9 \pm 81.3$  HV) compared with group B ( $382.8 \pm 51.1$  HV) or group C ( $271.7 \pm 41.9$  HV) ( $P < 0.05$ ) (**Figure 4E**). There was a significant difference between group B and group C. This indicated that group B had increased new bone formation. Group A gained more new bone than group B, thereby forming higher compressive strength. Thus, the EPCs added to group A provided the blood supply, which may be a favorable environment for dental implantation.

### Micro-CT evaluation

The associated microarchitecture parameters obtained from micro-CT clearly depicted the differences among the three groups (**Figure 5**). Group A showed the highest values in BV/TV (1.38-fold), Tb.Th (1.24-fold), Tb.N (1.27-fold) and a moderately decreased Tb.Sp (74.9%) compared with group B. The mean value of Conn.Dn in group A was significantly higher than group C, but lower than group B. Group B exhibited a bigger effect than group C, with a markedly increased BV/TV (1.4-fold), Conn.Dn (2.36-fold), Tb.Th (1.18-fold), and Tb.N (1.6-fold) and a decreased Tb.Sp (77.5%).

### Fluorochrome microscopy

The deposition of mineralized bone matrix and dynamic histomorphometric parameters were demonstrated at 4, 12, and 20 weeks through measurement of fluorescent labeling (**Figure 6A-C**). At 4-12 weeks post-operation, the mineral apposition rate was significantly higher in group A ( $1.68 \pm 0.15$   $\mu\text{m}/\text{day}$ ) than group B ( $1.15 \pm 0.18$   $\mu\text{m}/\text{day}$ ) or group C ( $0.87 \pm 0.14$   $\mu\text{m}/\text{day}$ ). Nevertheless, at 12-20 weeks post-operation, differences in mineral apposition rates among the three groups were not statistically significant ( $P > 0.05$ ) (**Figure 6D**).

### Histological observation

The decalcified sections stained with hematoxylin-eosin were observed under light microscopy (**Figure 7A1, 7A2, 7B1, 7B2, 7C1, 7C2**). All three groups showed no evidence of inflamma-

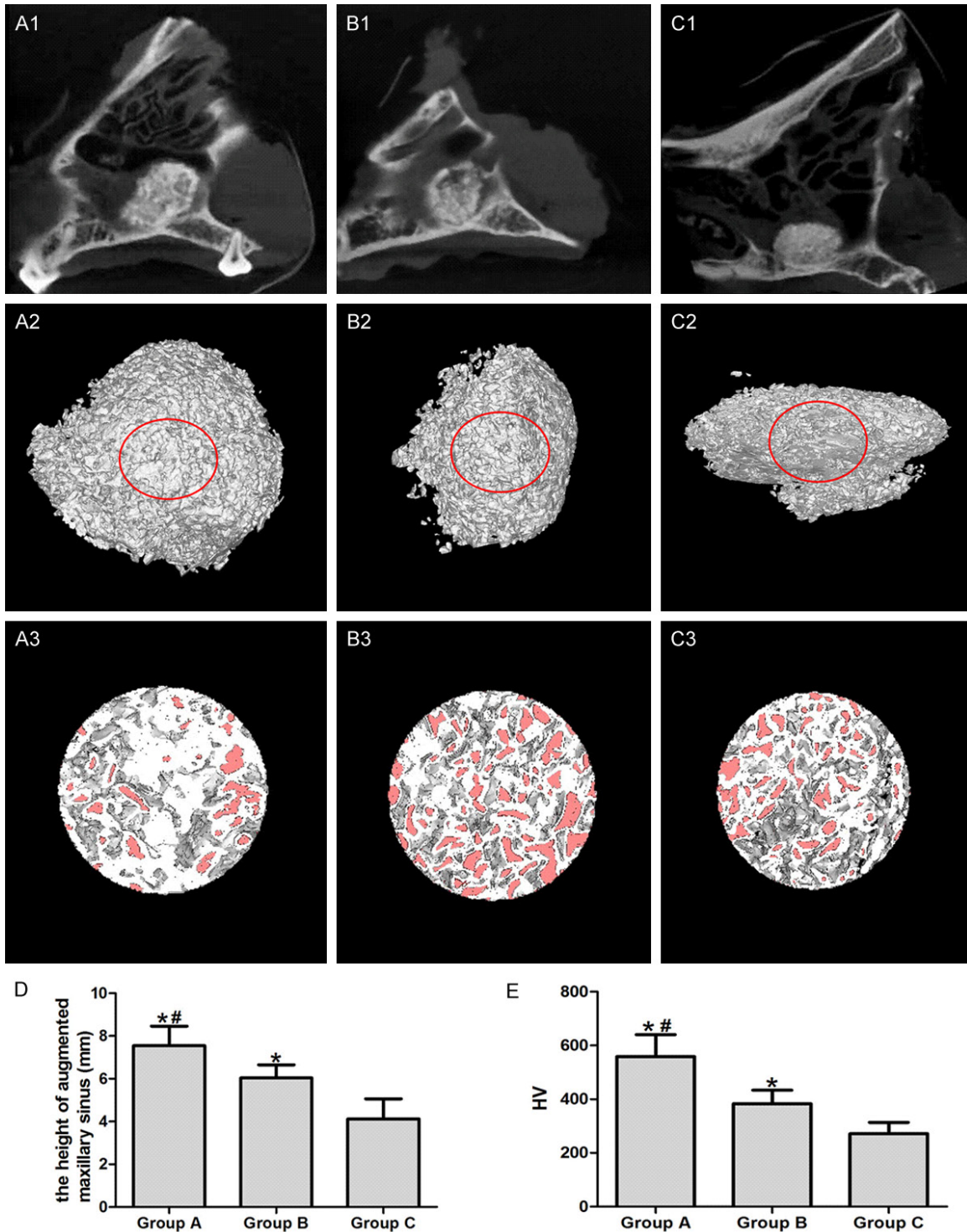


**Figure 4.** The augmented maxillary sinus of each group at 24 weeks post-operation shown by sagittal maxillofacial CT images (A1: group A, B1: group B, C1: group C). 3-D-micro-CT images of the total mineralized volume in groups A, B, and C were also displayed (A2: group A, B2: group B, C2: group C). Three-dimensional reconstructed images of the volume of interest (VOI) for the three groups represent remnants of Bio-Oss granules (pink) and newly formed bone (white) (A3: group A, B3: group B, C3: group C). (D) The mean height value and (E) the microhardness of each group was measured. Each value was expressed as mean  $\pm$  SD. \*:  $P \leq 0.05$  vs group C, #:  $P \leq 0.05$  vs group B. Group A contained scaffold Bio-Oss/MSCs-derived osteogenic cells and EPCs ( $n = 3$ ); Group B contained scaffold Bio-Oss/MSCs-derived osteogenic cells ( $n = 3$ ) as a control group; Group C contained scaffold Bio-Oss/EPCs ( $n = 3$ ) as a control group.

## Endothelial progenitor cells with stem cells improve osteogenesis

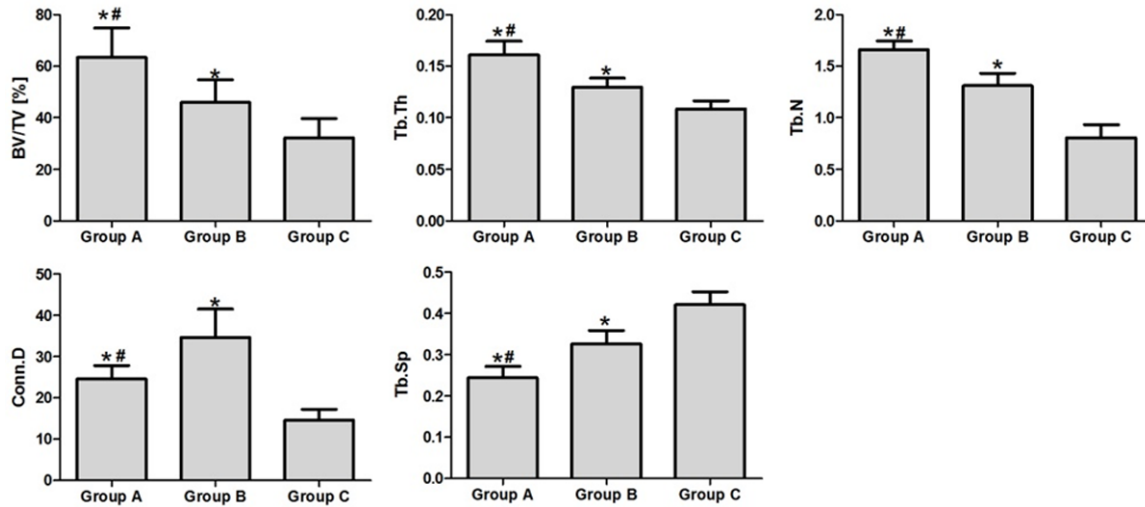


**Figure 5.** The 3-D microarchitectural indices analyzed using micro-CT: total volume ratio (BV/TV), connectivity density (Conn.Dn), trabecular thickness (Tb.Th), trabecular separation (Tb.Sp), and trabecular number (Tb.N). Data are expressed as mean  $\pm$  SD. \*:  $P \leq 0.05$  vs group C, #:  $P \leq 0.05$  vs group B.

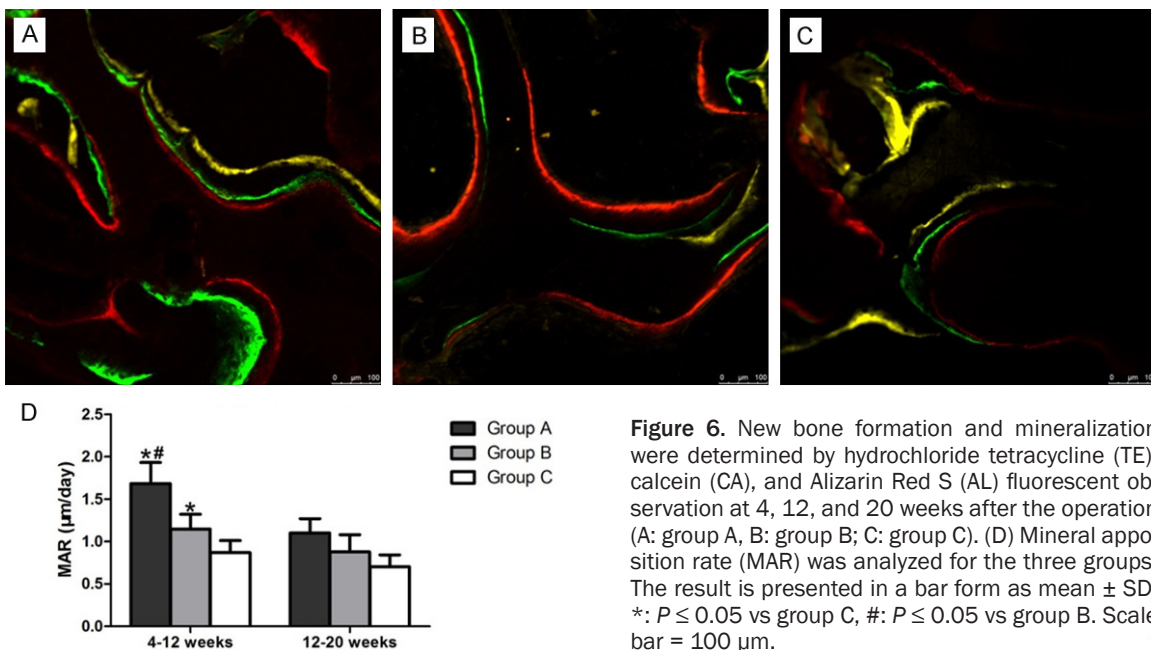


**Figure 6.** New bone formation and mineralization were determined by hydrochloride tetracycline (TE), calcein (CA), and Alizarin Red S (AL) fluorescent observation at 4, 12, and 20 weeks after the operation (A: group A, B: group B; C: group C). (D) Mineral apposition rate (MAR) was analyzed for the three groups. The result is presented in a bar form as mean  $\pm$  SD. \*:  $P \leq 0.05$  vs group C, #:  $P \leq 0.05$  vs group B. Scale bar = 100  $\mu\text{m}$ .

tion and histological analysis revealed active bony regeneration in these grafted sinuses 24 weeks after surgery. The Bio-Oss granules could be easily identified by their color and shape. The newly formed bone lamellae surrounded the residual Bio-Oss granules and osteocytes were found in the bone lacunae. With high magnification, bone marrow was often observed in group A, but not in group B and group C. Multinucleated giant cells were found on the remnant particles' surface in

group C, but rarely detected in group A and group B. In addition, representative images at higher magnification in group A exhibited compact bone with many osteoblasts (Figure 8A). This result was further confirmed by osteocalcin antibody (OCN) immunohistochemistry detection (Figure 7A3, 7B3, 7C3). The stained area was bigger in group A than group B or group C. In addition, some blood vessels were found near the new bone and the remnant particles (Figure 8B).

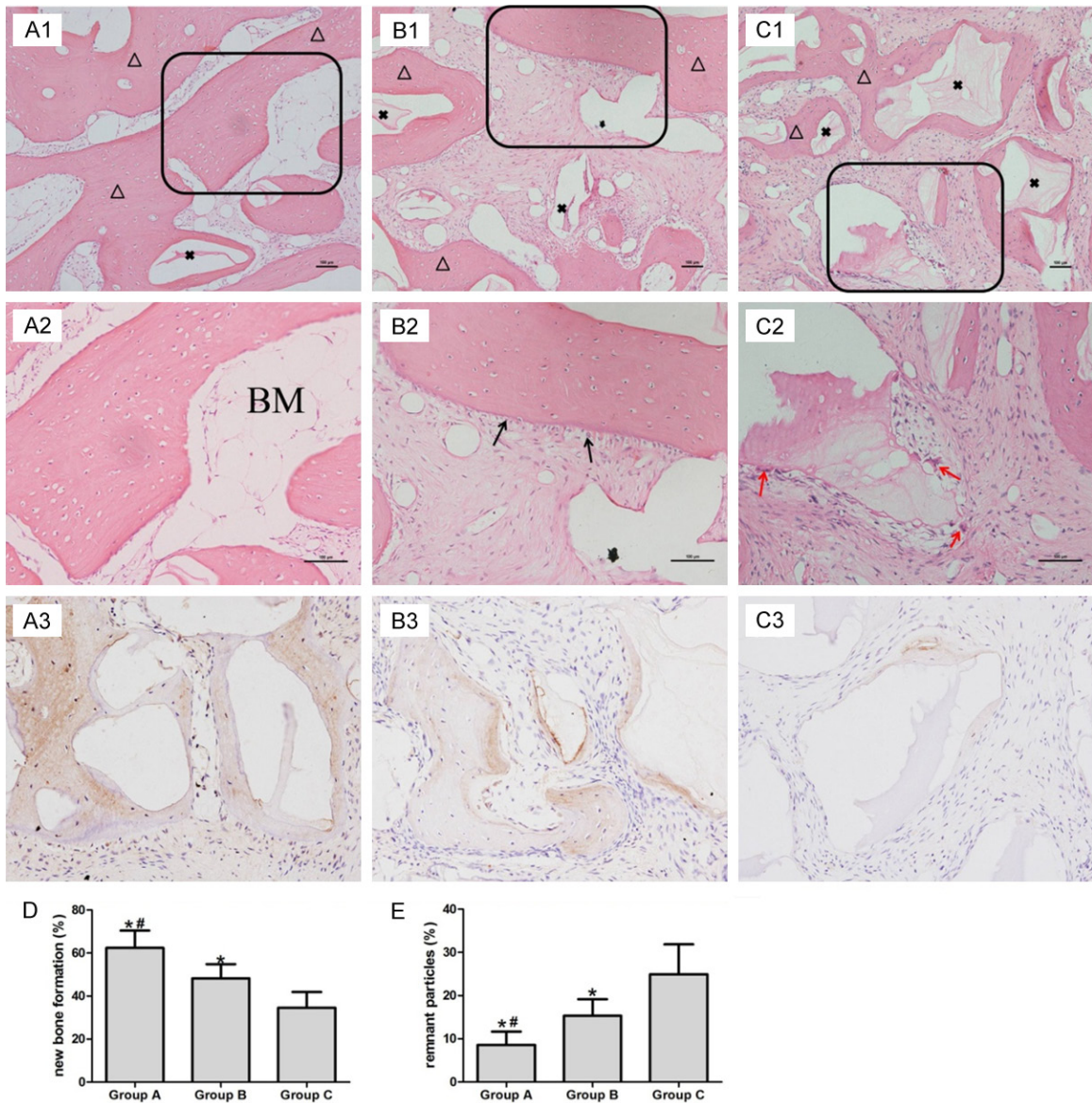


**Figure 7.** Representative histological sections of bone formation in augmented maxillary sinus in three groups. (A1) Group A contained scaffold Bio-Oss/MSCs-derived osteogenic cells and EPCs; (B1) Group B contained scaffold Bio-Oss/MSCs-derived osteogenic cells; (C1) Group C contained scaffold Bio-Oss and EPCs. A2 (group A), B2 (group B), and C2 (group C) show higher magnification images. Bone marrow was found in group A (A2). \*: residual Bio-Oss particles; Δ: the newly formed bone; black arrow: osteoblasts; red arrow: multinucleated giant cells. Scale bar = 100 μm. Osteocalcin (OCN) immunohistochemistry detection (A3: group A, B3: group B, C3: group C). (D, E) The new bone formation and remnant particles are shown. Each value is expressed as mean ± SD. \*:  $P \leq 0.05$  vs group C, #:  $P \leq 0.05$  vs group B.

In general, new bone formation in group A ( $62.37 \pm 8.07\%$ ) was significantly higher than in group B ( $48.2 \pm 6.63\%$ ) or group C ( $34.5 \pm 7.34\%$ ) (Figure 7D). Moreover, in group A, the mineralized tissue was observed not only at the surface, but also in the center of the specimen. This result was consistent with Micro-CT evaluation. In groups B and C, the newly formed bone

mostly showed at the surface layer of the specimen, but was not significant in the central region. The remnant particles in the three groups were also calculated. The results showed that residual particles in group C ( $25.43 \pm 6.02\%$ ) were more than group A ( $8.59 \pm 3.08\%$ ) or group B ( $15.32 \pm 3.82\%$ ) (Figure 7E) ( $P \leq 0.05$ ).

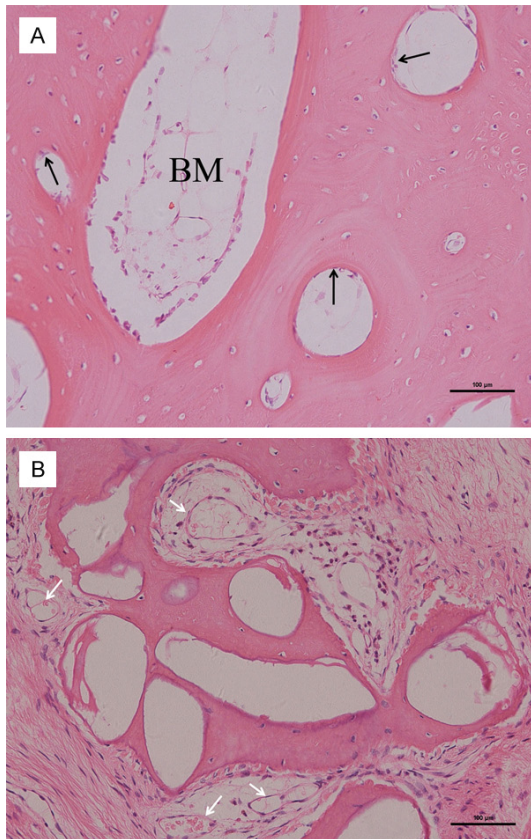


**Figure 8.** Representative histological sections in group A. (A) A compact bone area in an active phase with osteoblasts and blood vessels near the (B) newly formed bone. black arrow: osteoblasts; white arrow: blood vessels. Scale bar = 100 μm.

### Discussion

The sinus augmentation technique involves raising the sinus mucous membrane and filling the cavity with a grafting material to increase bone height in the posterior maxilla and provide adequate support for implants [22, 23]. These grafting materials should be biocompatible, similar to the natural bone in microstructure and composition [24, 25]. Moreover, they should serve as a proper matrix for cell growth and bone deposition [25-27]. In this study, through the scanning electron microscopy observations, MSCs-derived osteogenic cells and EPCs on the Bio-Oss granules had good growth. ALP activity confirmed that Bio-Oss granules did not affect the osteogenesis of MSCs. Therefore, Bio-Oss granules used in this study are reasonable for cell growth and bone deposition.

Bone graft materials are cell-free and osteoconductive [28]. However, bone regeneration

requires a long time, which limits the clinical use for sinus augmentation [29]. The engineering of bone tissue offers a new therapeutic strategy. Previous osteogenesis research concentrated on the function of the osteoblast or MSCs. However, the development of microvasculature is critical for the regeneration of bone. EPCs are considered candidates for vascular regeneration [30, 31]. Bone is a complex tissue and it is expected that the co-culture system may mimic more closely the *in vivo* environment, which is more conducive to osteogenesis than single-cell cultures [32, 33]. Transplantation of cell sheets containing EPCs and MSCs promotes bone regeneration *in vitro* and in rats [34-37]. In addition, the co-culture of rEPCs and rMSCs on needle-like calcium deficient hydroxyapatite results in early upregulation of osteogenic modulators [38]. In this experiment, we established the co-culture system of MSC-derived osteogenic cells and EPCs. Both MSCs and EPCs were from canine bone marrow. Thus, they shared their origin in the same niche where they could easily interact with each other [39].

With direct cell contact, crosstalk communication between MSC-derived osteogenic cells and EPCs occurred. Through the cell seeding efficiency on the Bio-Oss granules, we observed the co-cultured group obtained the highest cell adhesion. EPCs/MSCs can lead to proangiogenic differentiation and induce strong up-regulation of endothelial cell-cell adhesion proteins such as VE-cadherin and PECAM-1 [40]. Some MSCs may differentiate into endothelial-like cells, secrete more adhesion proteins, and promote cell retention and osteogenic differentiation of the stromal vascular fraction [41]. For the above reasons, the co-cultured system may provide an environment that favors cell adhesion. We also assessed cell osteogenesis on the Bio-Oss granules through ALP activity. The co-cultured group more easily stimulated ALP activity and EPCs alone did not have osteogenic ability. EPCs could release some growth factors continuously, such as VEGF and IGF-1, that recruit stem cells and direct them towards osteoblast differentiation [42, 43]. The co-cultured system may induce osteogenic differentiation of MSCs. However, it is still unclear whether co-autotransplantation of EPCs with MSCs promotes better bone regeneration *in vivo* for sinus augmentation. Large-animal models are suggested before a clinical application to evaluate the effect of the bone grafts [44]. In this

## Endothelial progenitor cells with stem cells improve osteogenesis

study, we chose Bio-Oss granules with EPCs/ MSCs to elevate the maxillary sinus floor in the canine model.

CBCT images showed the augmented maxillary sinus at 24 weeks post-operation. The co-cultured group maintained the height of the augmented maxillary sinus compared to Bio-Oss granules with MSCs alone or EPCs alone, which was consistent with manual measurements of the specimens. Due to the low radiopacity value of Bio-Oss, it was not possible to differentiate the osteogenesis of three groups by means of Cone beam CT [45]. Micro-CT is a relatively rapid technique that permits quantitative morphometry of the bone in 3D [46]. The associated microarchitecture parameters reflected more new bone formation in group A, which could further be confirmed by hematoxylin-eosin staining and OCN immunohistochemistry. Moreover, 3D reconstruction of the VOI and histomorphometric measurements showed new bone formation increased in the central area of the graft in group A more than in groups B or C. It demonstrated that EPCs might effectively promote osteogenesis in tissue-engineered bone. In this study, the origin of the newly formed blood vessels was not clear. However, histological observation explicitly displayed more vessels near the new bone in group A. Transplanted EPCs could be recruited to the osseous fracture in the healing environment and enhance angiogenesis and osteogenesis [47]. In group A, it is possible that EPCs formed the capillary-like structures throughout the graft and participated in the bone regeneration. The neovascularization may facilitate the supply of oxygen and nutrition for the graft, thereby possibly contributing to the height of the augmented maxillary sinus. Because of relying on host blood vessel growth, group B did not acquire sufficient nutrition for new bone formation. Group C, namely Bio-Oss with EPCs, had less bone formation using only an osteoconduction process. Moreover, this group had the least migrated osteoblasts and vascular cells from recipient tissue and less new bone was formed at the center of the graft.

Fluorochrome labeling histomorphometrical change analysis by confocal laser scanning microscope demonstrated that the process of the bone deposition was accelerated by the transplanted EPCs, especially at 4-12 weeks post-operation, which was consistent with ALP

activity *in vitro*. The earlier bone regeneration may withstand continuous air pressure in the maxillary sinus, thereby maximally maintaining the height of the augmented sinus and increasing the compressive strength [48]. The mechanism may underlie a direct or indirect role of VEGF in this study. In previous research, the expression of VEGF was improved in the co-culture system *in vitro* [40]. VEGF is essential for endochondral bone formation [49]. Because of nutrition and signaling interaction between endothelial cells and MSCs, VEGF-induced angiogenesis may accelerate differentiation of MSCs [50]. Thus, more OCN-positive osteoblasts were detected in group A. Hematoxylin-eosin sections showed compact bone with many osteoblasts and bone marrow in group A. In another words, more mature bone was formed. Hence, group A exhibited the highest compressive strength, suggesting the co-culture will be beneficial for dental implantation.

Bone remodeling includes resorption of pre-existing bone tissue by osteoclasts and new bone formation by osteoblasts [51]. The blood vessels involved in bone resorption and deposition regulate the activities of osteoclasts and osteoblasts. Thus, in this study, the Bio-Oss remnant particles were less in group A compared with groups B or C. Besides, the value of Conn.Dn in group A was inferior to group B by micro CT, which may be also related to the rapid material degradation. In addition, multinucleated giant cells were found on the remnant particles surface in group C, possibly because of the higher amount of remaining bone material.

EPCs have been successfully isolated from bone marrow, peripheral blood, and umbilical cord blood [52]. Consistent with our results, EPCs as seed cells combined with BMSCs can promote vascularization and osteogenesis of tissue-engineered bone in Beagle dogs [53]. However, it is still unclear which cell source and co-culture ratio would enhance vascularization in the engineering of bone tissue. Hence, it is necessary to do more *in vivo* experiments.

In conclusion, the results suggested that co-autotransplantation of bone marrow-EPCs with MSCs can significantly enhance the *in vivo* osteogenic efficacy and prevent necrosis in a sinus augmentation model in dogs. The co-culture system may recreate more closely the *in vivo* environment than single cell culture. This

## Endothelial progenitor cells with stem cells improve osteogenesis

tissue engineered bone may be broadly useful in maxillary sinus augmentation, thus reducing the failure of implant surgery.

### Acknowledgements

This work was supported by grants from the Shanghai Municipal Health Commission Youth Fund (grant no. 20184Y0021), Youth Natural Science Foundation Project, School & Hospital of Stomatology, Tongji University (grant no. 20-187002), National Natural Science Foundation of China (grant no. 81670962), Key Research and Development Program of the Ministry of science and technology of China -- Key Special Project (2019.08-2023.07).

### Disclosure of conflict of interest

None.

**Address correspondence to:** Zuolin Wang, Department of Oral Implantology, School & Hospital of Stomatology, Tongji University, Shanghai Engineering Research Center of Tooth Restoration and Regeneration, Shanghai 200072, China. Tel: +86-021-66315500; E-mail: zuolinwang2013@126.com

### References

- [1] Park JB. Use of cell-based approaches in maxillary sinus augmentation procedures. *J Craniofac Surg* 2010; 21: 557-560.
- [2] Jensen OT, Shulman LB, Block MS and Iacono VJ. Report of the sinus consensus conference of 1996. *Int J Oral Maxillofac Implants* 1998; 13 Suppl: 11-45.
- [3] Zizelmann C, Schoen R, Metzger MC, Schmelzeisen R, Schramm A, Dott B, Bormann KH and Gellrich NC. Bone formation after sinus augmentation with engineered bone. *Clin Oral Implants Res* 2007; 18: 69-73.
- [4] Chiapasco M, Casentini P and Zaniboni M. Bone augmentation procedures in implant dentistry. *Int J Oral Maxillofac Implants* 2009; 24 Suppl: 237-259.
- [5] Esposito M, Grusovin MG, Coulthard P and Worthington HV. The efficacy of various bone augmentation procedures for dental implants: a Cochrane systematic review of randomized controlled clinical trials. *Int J Oral Maxillofac Implants* 2006; 21: 696-710.
- [6] Piattelli M, Favero GA, Scarano A, Orsini G and Piattelli A. Bone reactions to anorganic bovine bone (Bio-Oss) used in sinus augmentation procedures: a histologic long-term report of 20 cases in humans. *Int J Oral Maxillofac Implants* 1999; 14: 835-840.
- [7] Weibrich G, Trettin R, Gnoth SH, Götz H, Duschner H and Wagner W. Determining the size of the specific surface of bone substitutes with gas adsorption. *Mund Kiefer Gesichtschir* 2000; 4: 148-152.
- [8] Degidi M, Artese L, Rubini C, Perrotti V, Iezzi G and Piattelli A. Microvessel density and vascular endothelial growth factor expression in sinus augmentation using Bio-Oss. *Oral Dis* 2006; 12: 469-475.
- [9] Springer IN, Nocini PF, Schlegel KA, De Santis D, Park J, Warnke PH, Terheyden H, Zimmermann R, Chiarini L, Gardner K, Ferrari F and Wiltfang J. Two techniques for the preparation of cell-scaffold constructs suitable for sinus augmentation: steps into clinical application. *Tissue Eng* 2006; 12: 2649-2656.
- [10] Yamada Y, Nakamura S, Ito K, Kohgo T, Hibi H, Nagasaka T and Ueda M. Injectable tissue-engineered bone using autogenous bone marrow-derived stromal cells for maxillary sinus augmentation: clinical application report from a 2-6-year follow-up. *Tissue Eng Part A* 2008; 14: 1699-1707.
- [11] Krebsbach PH, Kuznetsov SA, Bianco P and Robey PG. Bone marrow stromal cells: characterization and clinical application. *Crit Rev Oral Biol Med* 1999; 10: 165-181.
- [12] Kaigler D, Krebsbach PH, Wang Z, West ER, Horger K and Mooney DJ. Transplanted endothelial cells enhance orthotopic bone regeneration. *J Dent Res* 2006; 85: 633-637.
- [13] Asahara T, Murohara T, Sullivan A, Silver M, van der Zee R, Li T, Witzenbichler B, Schatteman G and Isner JM. Isolation of putative progenitor endothelial cells for angiogenesis. *Science* 1997; 275: 964-967.
- [14] Wu X, Rabkin-Aikawa E, Guleserian KJ, Perry TE, Masuda Y, Sutherland FW, Schoen FJ, Mayer JE and Bischoff J. Tissue-engineered microvessels on three-dimensional biodegradable scaffolds using human endothelial progenitor cells. *Am J Physiol Heart Circ Physiol* 2004; 287: H480-487.
- [15] Han Y and Hsieh FH. Osteogenic differentiation of late-outgrowth CD45-negative endothelial progenitor cells. *J Vasc Res* 2014; 51: 369-375.
- [16] Steiner D, Köhn K, Beier JP, Stürzl M, Horch RE and Arkudas A. Cocultivation of mesenchymal stem cells and endothelial progenitor cells reveals antiapoptotic and proangiogenic effects. *Cells Tissues Organs* 2017; 204: 218-227.
- [17] Kern S, Eichler H, Stoeve J, Klüter H and Bieback K. Comparative analysis of mesenchymal stem cells from bone marrow, umbilical cord blood, or adipose tissue. *Stem Cells* 2006; 24: 1294-1301.
- [18] Haas R, Mailath G, Dörtbudak O and Watzek G. Bovine hydroxyapatite for maxillary sinus aug-

## Endothelial progenitor cells with stem cells improve osteogenesis

- mentation: analysis of interfacial bond strength of dental implants using pull-out tests. *Clin Oral Implants Res* 1998; 9: 117-122.
- [19] Ohya M, Yamada Y, Ozawa R, Ito K, Takahashi M and Ueda M. Sinus floor elevation applied tissue-engineered bone. Comparative study between mesenchymal stem cells/platelet-rich plasma (PRP) and autogenous bone with PRP complexes in rabbits. *Clin Oral Implants Res* 2005; 16: 622-629.
- [20] Giavaresi G, Fini M, Cigada A, Chiesa R, Rondelli G, Rimondini L, Aldini NN, Martini L and Giardino R. Histomorphometric and microhardness assessments of sheep cortical bone surrounding titanium implants with different surface treatments. *J Biomed Mater Res A* 2003; 67: 112-120.
- [21] Ma YY, Sun D, Li J and Yin ZC. Transplantation of endothelial progenitor cells alleviates renal interstitial fibrosis in a mouse model of unilateral ureteral obstruction. *Life Sci* 2010; 86: 798-807.
- [22] Palma VC, Magro-Filho O, de Oliveria JA, Lundgren S, Salata LA and Sennerby L. Bone reformation and implant integration following maxillary sinus membrane elevation: an experimental study in primates. *Clin Implant Dent Relat Res* 2006; 8: 11-24.
- [23] Sauerbier S, Stubbe K, Maglione M, Haberstroh J, Kuschnierz J, Oshima T, Xavier SP, Brunenberg L, Schmelzeisen R and Gutwald R. Mesenchymal stem cells and bovine bone mineral in sinus lift procedures—an experimental study in sheep. *Tissue Eng Part C Methods* 2010; 16: 1033-1039.
- [24] Wei J, Liu CS, Hong H, Yuan Y and Chen FP. Study on a new type of biodegradable calcium phosphate cement porous scaffold. *Journal of Inorganic Materials* 2006; 4: 958-964.
- [25] Wiedmann-Al-Ahmad M, Gutwald R, Gellrich NC, Hübner U and Schmelzeisen R. Search for ideal biomaterials to cultivate human osteoblast-like cells for reconstructive surgery. *J Mater Sci Mater Med* 2005; 16: 57-66.
- [26] Roach P, Eglin D, Rohde K and Perry CC. Modern biomaterials: a review - bulk properties and implications of surface modifications. *J Mater Sci Mater Med* 2007; 18: 1263-1277.
- [27] Graziano A, d'Aquino R, Cusella-De Angelis MG, De Francesco F, Giordano A, Laino G, Piatelli A, Traini T, De Rosa A and Papaccio G. Scaffold's surface geometry significantly affects human stem cell bone tissue engineering. *J Cell Physiol* 2008; 214: 166-172.
- [28] Al Ruhaimi KA. Bone graft substitutes: a comparative qualitative histologic review of current osteoconductive grafting materials. *Int J Oral Maxillofac Implants* 2001; 16: 105-114.
- [29] Aghaloo TL and Moy PK. Which hard tissue augmentation techniques are the most successful in furnishing bony support for implant placement. *Int J Oral Maxillofac Implants* 2007; 22 Suppl: 49-70.
- [30] Sepúlveda P, Martínez-León J and García-Verdugo JM. Neovascularization with endothelial precursors for the treatment of ischemia. *Transplant Proc* 2007; 39: 2089-2094.
- [31] Qin Y and Zhang C. Endothelial progenitor cell-derived extracellular vesicle-mediated cell-to-cell communication regulates the proliferation and osteoblastic differentiation of bone mesenchymal stromal cells. *Mol Med Rep* 2017; 16: 7018-7024.
- [32] Choong CS, Huttmacher DW and Triffitt JT. Co-culture of bone marrow fibroblasts and endothelial cells on modified polycaprolactone substrates for enhanced potentials in bone tissue engineering. *Tissue Eng* 2006; 12: 2521-2531.
- [33] Chen L, Wu J, Wu C, Xing F, Li L, He Z, Peng K and Xiang Z. Three-dimensional co-culture of peripheral blood-derived mesenchymal stem cells and endothelial progenitor cells for bone regeneration. *J Biomed Nanotechnol* 2019; 15: 248-260.
- [34] Liang Y, Wen L, Shang F, Wu J, Sui K and Ding Y. Endothelial progenitors enhanced the osteogenic capacities of mesenchymal stem cells in vitro and in a rat alveolar bone defect model. *Arch Oral Biol* 2016; 68: 123-130.
- [35] Liu H, Jiao Y, Zhou W, Bai S, Feng Z, Dong Y, Liu Q, Feng X and Zhao Y. Endothelial progenitor cells improve the therapeutic effect of mesenchymal stem cell sheets on irradiated bone defect repair in a rat model. *J Transl Med* 2018; 16: 137.
- [36] Liu H, Zhou W, Ren N, Feng Z, Dong Y, Bai S, Jiao Y, Wang Z and Zhao Y. Cell Sheets of co-cultured endothelial progenitor cells and mesenchymal stromal cells promote osseointegration in irradiated rat bone. *Sci Rep* 2017; 7: 3038.
- [37] Li Q and Wang Z. Influence of mesenchymal stem cells with endothelial progenitor cells in co-culture on osteogenesis and angiogenesis: an in vitro study. *Arch Med Res* 2013; 44: 504-513.
- [38] Sadowska JM, Guillem-Marti J and Ginebra MP. The influence of physicochemical properties of biomimetic hydroxyapatite on the in vitro behavior of endothelial progenitor cells and their interaction with mesenchymal stem cells. *Adv Healthc Mater* 2019; 8: e1801138.
- [39] Dazzi F, Ramasamy R, Glennie S, Jones SP and Roberts I. The role of mesenchymal stem cells in haemopoiesis. *Blood Rev* 2006; 20: 161-171.
- [40] Aguirre A, Planell JA and Engel E. Dynamics of bone marrow-derived endothelial progenitor cell/mesenchymal stem cell interaction in co-

## Endothelial progenitor cells with stem cells improve osteogenesis

- culture and its implications in angiogenesis. *Biochem Biophys Res Commun* 2010; 400: 284-291.
- [41] Harvestine JN, Orbay H, Chen JY, Sahar DE and Leach JK. Cell-secreted extracellular matrix, independent of cell source, promotes the osteogenic differentiation of human stromal vascular fraction. *J Mater Chem B* 2018; 6: 4104-4115.
- [42] Tarkka T, Sipola A, Jämsä T, Soini Y, Ylä-Herttuala S, Tuukkanen J and Hautala T. Adenoviral VEGF-A gene transfer induces angiogenesis and promotes bone formation in healing osseous tissues. *J Gene Med* 2003; 5: 560-566.
- [43] Belfiore A, Frasca F, Pandini G, Sciacca L and Vigneri R. Insulin receptor isoforms and insulin receptor/insulin-like growth factor receptor hybrids in physiology and disease. *Endocr Rev* 2009; 30: 586-623.
- [44] Aral A, Yalçın S, Karabuda ZC, Anil A, Jansen JA and Mutlu Z. Injectable calcium phosphate cement as a graft material for maxillary sinus augmentation: an experimental pilot study. *Clin Oral Implants Res* 2008; 19: 612-617.
- [45] Pekkan G, Aktas A and Pekkan K. Comparative radiopacity of bone graft materials. *J Cranio-maxillofac Surg* 2012; 40: e1-4.
- [46] Butz F, Ogawa T, Chang TL and Nishimura I. Three-dimensional bone-implant integration profiling using micro-computed tomography. *Int J Oral Maxillofac Implants* 2006; 21: 687-695.
- [47] Matsumoto T, Kawamoto A, Kuroda R, Ishikawa M, Mifune Y, Iwasaki H, Miwa M, Horii M, Hayashi S, Oyamada A, Nishimura H, Murasawa S, Doita M, Kurosaka M and Asahara T. Therapeutic potential of vasculogenesis and osteogenesis promoted by peripheral blood CD34-positive cells for functional bone healing. *Am J Pathol* 2006; 169: 1440-1457.
- [48] Wang S, Zhang Z, Xia L, Zhao J, Sun X, Zhang X, Ye D, Uludağ H and Jiang X. Systematic evaluation of a tissue-engineered bone for maxillary sinus augmentation in large animal canine model. *Bone* 2010; 46: 91-100.
- [49] Gerber HP, Vu TH, Ryan AM, Kowalski J, Werb Z and Ferrara N. VEGF couples hypertrophic cartilage remodeling, ossification and angiogenesis during endochondral bone formation. *Nat Med* 1999; 5: 623-628.
- [50] Wozney JM. The bone morphogenetic protein family and osteogenesis. *Mol Reprod Dev* 1992; 32: 160-167.
- [51] Barou O, Mekraldi S, Vico L, Boivin G, Alexandre C and Lafage-Proust MH. Relationships between trabecular bone remodeling and bone vascularization: a quantitative study. *Bone* 2002; 30: 604-612.
- [52] Kim S and von RH. Endothelial stem cells and precursors for tissue engineering: cell source, differentiation, selection, and application. *Tissue Eng Part B Rev* 2008; 14: 133-147.
- [53] Wu XW, Yin J and Wei YX. Effects of endothelial progenitor cells on vascularization and osteogenesis of tissue-engineered bones in beagle dogs. *Zhongguo Yi Xue Ke Xue Yuan Xue Bao* 2018; 40: 642-650.